Effect of chloride concentration range on the corrosion resistance of Cu–xNi alloys

I. MILOŠEV[1] and M. METIKOŠ-HUKOVIĆ[2]

[1]*J. Stefan Institute, Jamova 39, 1001 Ljubljana, Slovenia;* [2]*Department of Electrochemistry, Faculty of Chemical Engineering and Technology, University of Zagreb, Savska 16, 10000 Zagreb, Croatia*

The anodic behaviour of Cu–xNi alloys and Cu and Ni metals was studied in slightly alkaline solutions containing Cl^--ions in the concentration range from 0.01 to 2.0 mol dm^{-3}. The morphology and composition of the surface films formed by anodic polarization were analysed by scanning electron microscopy (SEM) and energy dispersive X-ray spectroscopy (EDS). On the basis of quasi-potentiodynamic polarization data, E_c against c_{NaCl} diagrams were constructed, where E_c is the critical pitting potential. These diagrams allow the determination of areas where the materials are susceptible to localized pitting attack. A critical chloride concentration (c_{crit}) exists below which the resistance to localized corrosion increases with decreasing nickel content and above which it increases with increasing nickel content. This effect is connected with the change in the corrosion resistance observed for the pure metal constituents, i.e., copper and nickel as a function of chloride concentration. The kinetic parameters of pitting corrosion of Cu–xNi alloys reflect the specific properties of both elements and suggest that an increase in Ni content above 40% would not have a significant effect on the corrosion resistance of Cu–xNi alloys.

Keywords: *copper, cu–xNi alloys, EDS, localized pitting attack, nickel, SEM*

1. Introduction

Copper–nickel (Cu–xNi) alloys are extensively used as condenser tube materials in saline environments [1–8] as well as catalysts for hydrogenation and dehydrogenation [9–12]. Several authors have shown that, as long as the nickel content in the alloy does not exceed 40 wt %, the passivity of copper–nickel alloys in chloride containing solutions is established by the formation of a duplex oxide film, consisting of an outer layer of cupric hydroxychloride, $Cu_2(OH)_3Cl$, overlying a compact inner Cu_2O layer [1–6]. Only in the case of Cu–40Ni alloy was nickel oxide identified as a major corrosion product [1]. The composition of the reaction product formed on Cu–Ni alloys is strongly potential dependent. At more active potentials, where preference for selective nickel dissolution is greater, the reaction product was found to contain nickel concentrations in excess of those in the bulk alloy [1]. At higher potentials nickel is depleted in the reaction product. The inner Cu_2O layer is able to incorporate foreign cations, i.e. nickel [1–6], as well as iron [5–7], which affects its protective properties. Consequently, copper-nickel alloys were found to exhibit improved corrosion characteristics compared to copper [4]. With increasing nickel content in the alloy the corrosion resistance increases [1, 2, 4]. North and Pryor suggested that nickel ions incorporated in the defect lattice of Cu_2O decrease its ionic and electronic conductivity [1, 2]. When the nickel content in the alloy exceeds 40 wt %, however, nickel oxide becomes the major reaction product. Incorporation of cupric ions would not significantly change the electronic or ionic resistance of NiO, which implies that alloys containing 40 wt % of nickel should exhibit the optimal corrosion resistance [1, 2].

All the studies mentioned above were performed at a constant chloride concentration, that is, 3.4% NaCl solution [1, 3, 5, 6], 0.5 M NaCl [2] or natural sea water [4]. In our previous publications the behaviour of Cu–10Ni alloy in slightly alkaline solutions containing chloride ions has been extensively studied [13–15]. It was the aim of the present study to investigate systematically the corrosion resistance of a series of copper-nickel alloys in a wide range of chloride concentrations in a slightly alkaline solution, pH 9.2. Results show that the corrosion resistance of Cu–Ni alloys increases with increasing nickel content, as suggested by other authors, but only in a certain range of chloride concentrations.

2. Experimental details

Copper–nickel alloys with a Ni content from 10 to 40 wt % were prepared from pure Cu and Ni constituents. The metals were homogenised for 4 h at

350 °C, rolled and then annealed for 1 h at 650 °C. Samples, 15 mm in diameter and 2 mm thick, were abraded with fine emery papers, polished with alumina powder down to 0.05 μm, and finally rinsed with distilled water and acetone. Prepared samples were embedded in a Teflon holder, so that an area of 0.785 cm^2 was exposed to the solution. Carbon rods and a saturated calomel electrode (SCE) served as counterelectrode and reference electrode, respectively. Potentials in the text refer to the SCE scale. Measurements were performed in borate buffer, pH 9.2, with and without addition of NaCl. The influence a NaCl addition was studied in the concentration range from 0.01 to 2.0 mol dm^{-3}. Measurements were carried out using a PAR&EGG model 273 potentiostat/galvanostat controlled by a PC. Potentiodynamic measurements were started −0.25 V with respect to the corrosion potential, E_{corr}, and progressed in the anodic direction with a potential scan rate of 0.3 mV s^{-1}. At least two measurements were performed and the mean value, the critical potential E_c, was then taken for further calculations. After electrochemical experiments the electrode surface was routinely checked by an Olympus SZH 10 Zoom stereo microscope. The morphology and composition of the films formed by electrochemical polarization were analyzed by scanning electron microscopy (SEM) and energy dispersive X-ray spectroscopy (EDS). A Joel JXA 840A SEM/EPMA instrument was used for this purpose.

3. Results and discussion

3.1. *Potentiodynamic polarization curves*

Anodic polarization curves recorded using a slow potential scan rate were employed to compare the behaviour of Cu and Ni and Cu–xNi alloys in chloride containing borate buffer solution, pH 9.2 (Figs 1–6). Curves were recorded for fourteen different concentrations of NaCl ranging from 0.01 to 2.0 mol dm^{-3}. In chloride-free solution the Tafel region of copper is followed by an anodic peak and a broad passive region extending up to 1.0 V (Fig. 1). It is well known that the passivity of copper is established due to the formation of a duplex oxide layer which consists of an outer CuO/Cu(OH)$_2$ layer and an inner barrier Cu$_2$O layer [12–15]. In the presence of chloride ions the passive layer is susceptible to localized breakdown, resulting in pitting corrosion attack. This process is reflected in several changes in the polarization curves. First, as the chloride concentration increases, the corrosion potential, E_{corr}, is shifted towards more negative values (from −0.08 to −0.3 V). In the presence of lower chloride concentrations the related current density increases but the passive range is still established. As the electrode potential exceeds a certain value, a steep increase in the current density is observed. This potential is denoted as the breakdown potential, E_b. The breakdown potential shifts towards more negative values as the chloride concentration increases. For chloride
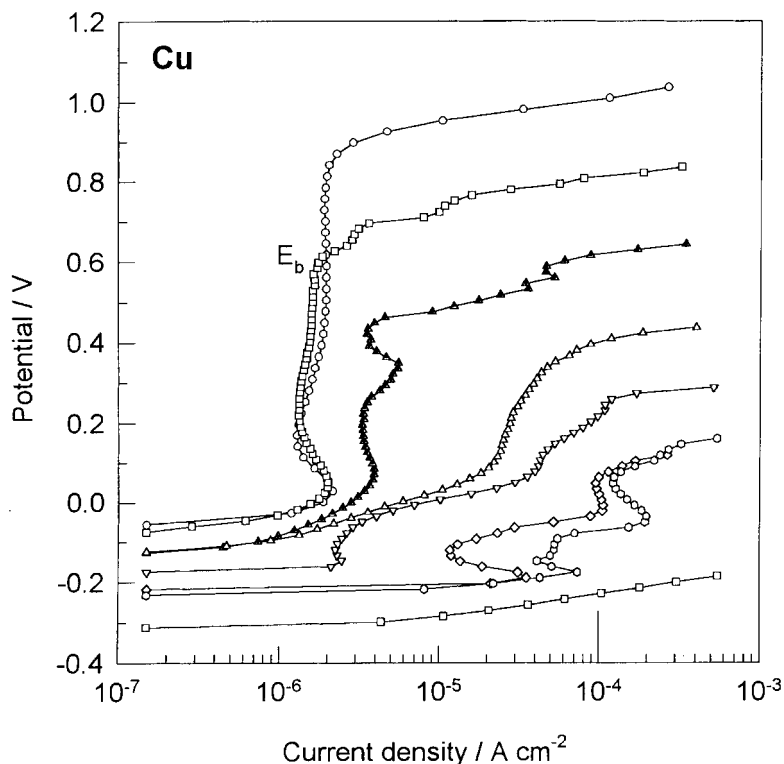

Fig. 1. Anodic polarization curves recorded for Cu metal in borate buffer containing various concentrations of NaCl: (○) 0, (□) 0.025, (△) 0.035, (▲) 0.05, (▽) 0.1, (◇) 0.3, (◯) 0.75 and (□) 2.0 M NaCl. Scan rate 0.3 mV s^{-1}.

concentrations higher than 0.025 mol dm^{-3}, a region of secondary passivity is observed. The term 'secondary passivity' is tentative due to the relatively high current densities (up to 2×10^{-4} A cm^{-2}). The span of this region becomes more pronounced with increasing chloride concentration. It is believed that this region corresponds to the formation of blue–green cupric oxychloride, as will be shown below. This product is obviously formed by a precipitation–dissolution mechanism. Its coverage of the electrode surface temporarily delays the current density increase, which then continues further as the electrode potential becomes more positive. For the highest chloride concentration investigated (2.0 mol dm^{-3}), copper shows no tendency towards passivation. Instead of localized corrosion the sample actually suffers general attack.

A quite different set of curves was recorded for nickel metal (Fig. 2). While in the chloride-free solution nickel shows a broad passive region extending up to approximately 0.9 V, the presence of only 0.01 mol dm^{-3} NaCl provokes localized breakdown of the passive film. The characteristic breakdown potential, E_b, already appears at 0.3 V. In contrast to copper, where the values of corrosion and breakdown potentials are extended over a broad potential region, an increase in chloride concentration transposes the corrosion and breakdown potentials of nickel only slowly in the negative direction.

Polarization curves for Cu–xNi alloys are presented in Figs 2–6. The general shape of the curves recorded for the Cu–10Ni alloy remains quite similar to that of copper metal. Although the values of cur-

rent density in the potential range of the anodic peak and in the passive range are lower than those of copper, breakdown potentials appear to be only slightly more positive. For concentrations lower than 0.2 mol dm^{-3} NaCl the shape of the polarization curves recorded for Cu–20Ni alloy is similar to that of copper and Cu–10Ni alloy. However, for higher chloride concentrations, the current density in the anodic peak decreases and, even for a concentration of 2.0 mol dm^{-3} NaCl, and active–passive transition peak is obtained. With increasing nickel content this behaviour becomes more pronounced. Whereas in the lower chloride concentration range Cu–30Ni and Cu–40Ni alloys exhibit breakdown potentials more negative than that of Cu–10Ni and Cu–20Ni alloys, the situation becomes just the opposite in the presence of higher chloride concentrations. Alloys containing higher nickel content now exhibit up to three orders of magnitude lower current density values compared to copper and Cu–10Ni alloy.

3.2. E_c vs c_{NaCl} diagrams

The results presented above clearly distinguish the effect of chloride concentration and that of nickel content on the corrosion resistance of Cu–Ni alloys. To characterize quantitatively the behaviour of these materials, the values of the critical potentials, E_c, are plotted against chloride concentration. These E_c against c_{NaCl} diagrams are presented in Fig. 7. Critical potentials are related to potential values at which the current density in the anodic polarization curves
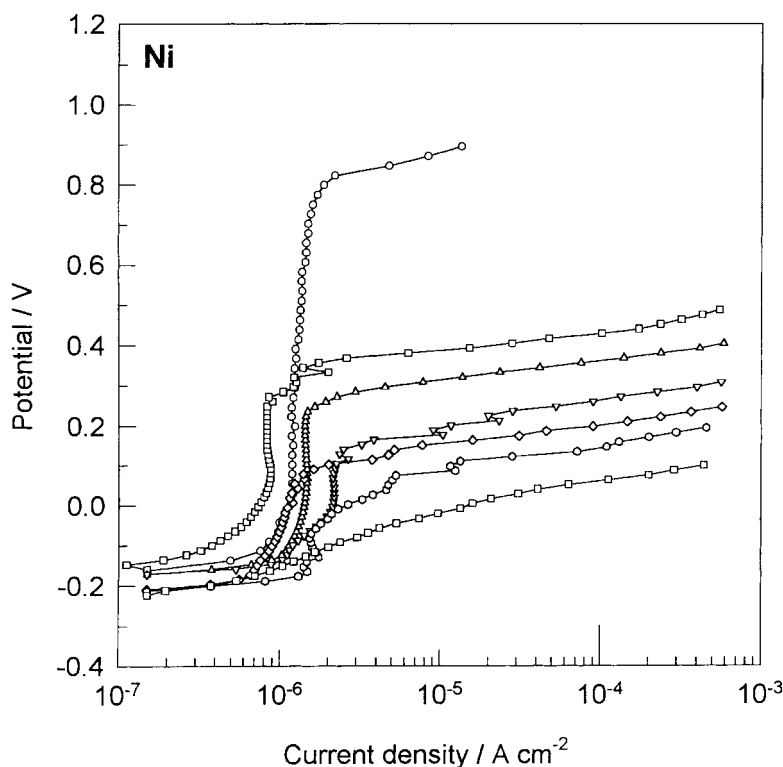

Fig. 2. Anodic polarization curves recorded for Ni metal in borate buffer containing various concentrations of NaCl. Scan rate was 0.3 mV s^{-1}. Symbol key as for Fig. 1.

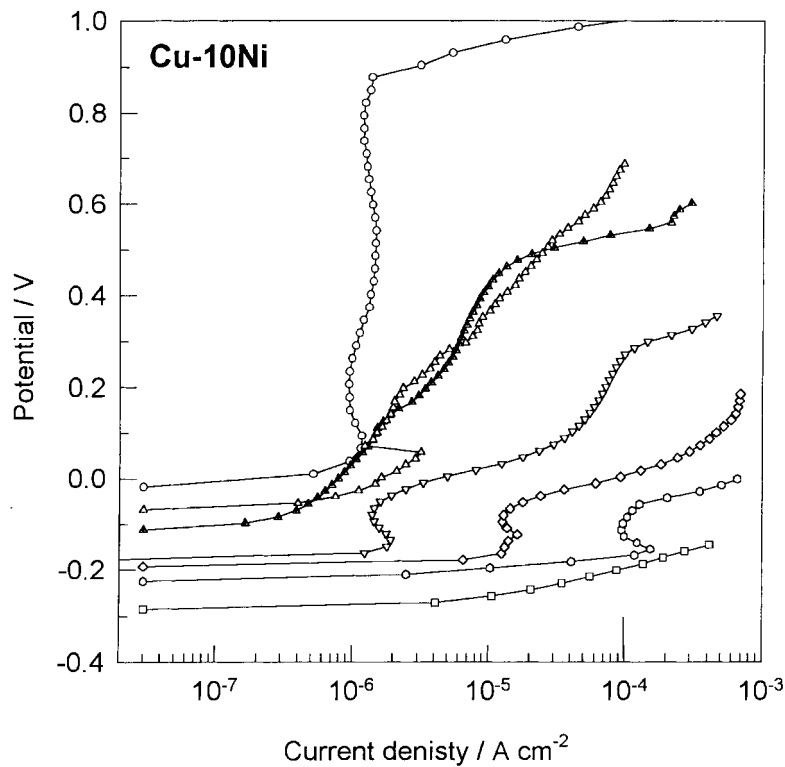Fig. 3. Anodic polarization curves recorded for Cu–10Ni alloy in borate buffer containing various concentrations of NaCl. Scan rate 0.3 mV s^{-1}. Symbol key as for Fig. 1.

reaches 10^{-4} A cm^{-2} (Figs 1–6). By choosing the reference current density value, a possible error in determination of the breakdown potentials as an intercept is avoided. It should be emphasised that the same trend is obtained in both cases (i.e., for E_b and

E_c). It is evident that in all cases a general relationship $E_c = a + b \log c_{NaCl}$ is established, although the constants a and b are strongly dependent on the chloride concentration range and nickel content in the alloy.
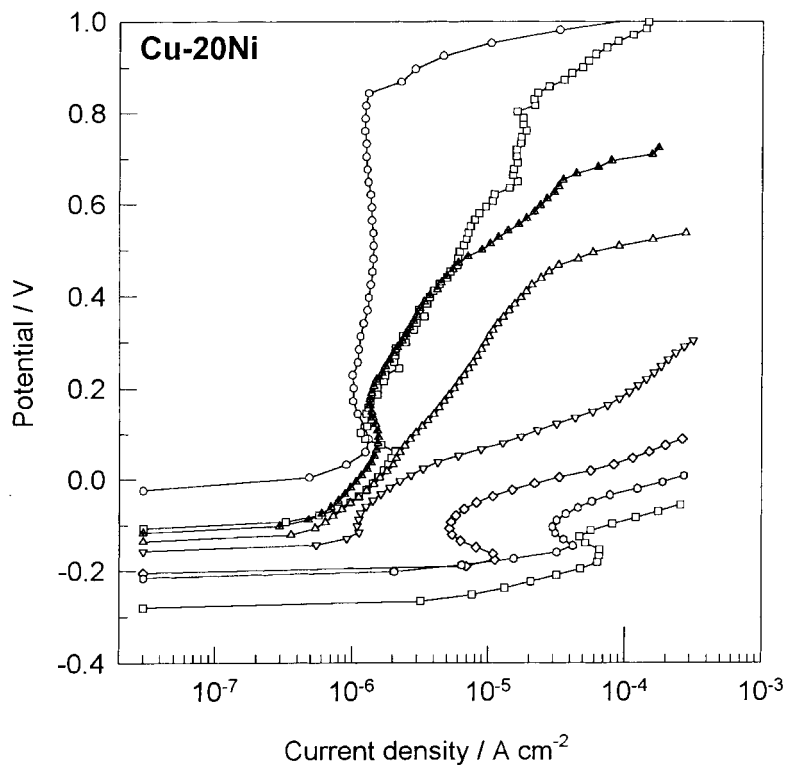

Fig. 4. Anodic polarization curves recorded for Cu–20Ni alloy in borate buffer containing various concentrations of NaCl. Scan rate 0.3 mV s^{-1}. Symbol key as for Fig. 1.
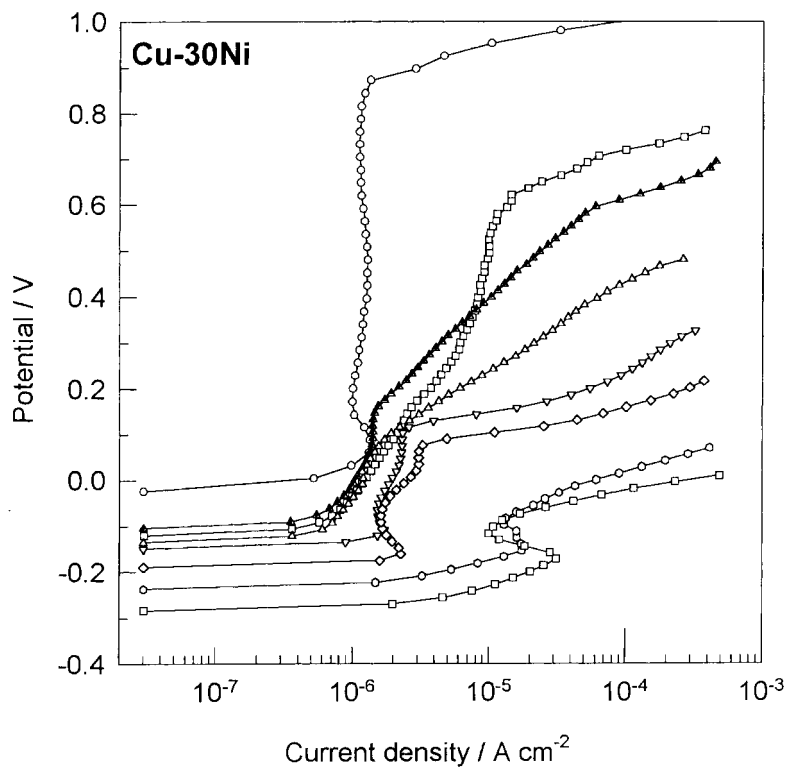
Fig. 5. Anodic polarization curves recorded for Cu–30Ni alloy in borate buffer containing various concentrations of NaCl. Scan rate 0.3 mV s^{-1}. Symbol key as for Fig. 1.

Up to 0.5 mol dm^{-3} NaCl the breakdown potential of copper shifts readily in the negative direction and the constant b amounts to -0.7 V dec^{-1} (Table 1). At higher chloride concentrations a break in this steep straight line occurs and the value of b decreases to

0.09 V dec^{-1}. Another limiting case, nickel metal, shows different behaviour. In the whole concentration range the constant b amounts to only -0.2 V dec^{-1}. It is evident that in the lower concentration range copper is superior to nickel in terms of resistance to localized
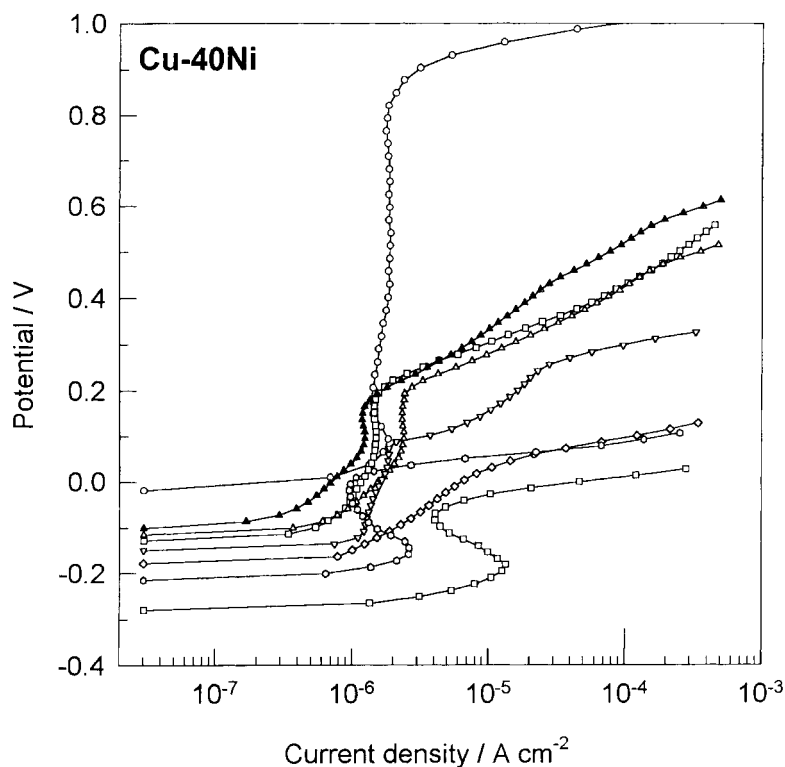
Fig. 6. Anodic polarization curves recorded for Cu–40Ni alloy in borate buffer containing various concentrations of NaCl. Scan rate 0.3 mV s^{-1}. Symbol key as for Fig. 1.

Table 1. Constants a and b of the general relationship $E_c = a + b \log c_{NaCl}$ *determined from polarization curves (Figs 1–6)*

E_c is the critical potential and c_{crit} is the chloride concentration at which the straight lines change their slope.

Sample	a	b	c_{crit}/M
Cu	−0.43	−0.70	⩽0.5
	−0.19	−0.09	⩾0.5
Cu–10Ni	−0.37	−0.68	⩽0.5
	−0.18	−0.11	⩾0.5
Cu–20Ni	−0.52	−0.78	⩽0.2
	−0.12	−0.22	⩾0.2
Cu–30Ni	−0.71	−0.85	⩽0.1
	−0.05	−0.21	⩾0.1
Cu–40Ni	−0.77	−0.84	⩽0.05
	0.03	−0.21	⩾0.05
Ni	0.10	−0.20	–

pitting attack. For example, in the presence of 0.01 mol dm^{-3} NaCl the value of E_c for copper is 0.5 V more positive (Fig. 7). As the chloride concentration increases, this difference decreases. In contrast to copper, the critical potentials of nickel move very slowly in the negative direction. The constant a corresponds to a chloride concentration of 1 mol dm^{-3}, and may be denoted as a standard critical potential (E_c^{θ}). The value of constant a is always more negative for copper than for nickel metal (Table 1).

From E_c against c_{NaCl} diagrams three important chloride concentrations are recognized. Straight lines of copper and nickel intersect at 0.1 mol dm^{-3} NaCl (Fig. 7). This chloride concentration is denoted as $c_{Cu/Ni}$. In the presence of higher chloride concentrations the resistance of nickel to pitting corrosion becomes superior to that of copper.

The second important parameter, denoted as the critical chloride concentration c_{crit}, denotes the chloride concentration at which the straight line $E_c = a + b \log c_{NaCl}$ changes slope. For chloride concentrations lower than the critical chloride concentrations ($c < c_{crit}$) the values of constant a shift readily towards more negative potentials with increasing nickel content from 10 to 40 wt % (Table 1). When the chloride concentration, however, exceeds the critical concentration ($c > c_{crit}$) the values of constant a move towards more positive potentials with increasing nickel content. Therefore the resistance to localized corrosion increases. In the concentration range $c < c_{crit}$ all copper–nickel alloys exhibit values of constant b similar to that of copper, that is, −0.68, −0.78, −0.85 and −0.84 V dec^{-1} (Table 1, Fig. 7). For higher chloride concentrations, however, the straight lines change their slopes, which now become similar to that of nickel metal, that is, −0.22 V dec^{-1} for Cu–20Ni, −0.21 V dec^{-1} for Cu-30Ni and −0.21 V dec^{-1} for Cu–40Ni and −0.20 V dec^{-1} for nickel.

It is noteworthy that an increase in nickel content above 40 wt % obviously has only a small effect on the improvement of the localized corrosion resistance. The constant a determined for nickel is only 70 mV more positive than that of Cu–40Ni alloy (Table 1). This result indirectly corroborates the hypothesis suggested by North and Pryor that an increase in nickel content above 40 wt % would not have a significant effect on the corrosion resistance of Cu–xNi alloys [1, 2].

The values of c_{crit} decrease with increasing nickel content in the alloy, that is, from 0.5 mol dm^{-3} for Cu–10Ni, 0.2 mol dm^{-3} for Cu–20Ni, 0.1 mol dm^{-3} for Cu–30Ni to 0.05 mol dm^{-3} for Cu–40Ni alloy. Therefore, with increasing nickel content in the alloy, the critical chloride concentration above which the alloy behaves similarly to nickel metal decreases.

The third significant parameter which can be determined from E_c against c_{NaCl} diagrams is denoted as $c_{alloy/Ni}$ (Fig. 7). It is related to the chloride concentration at which the straight line of a particular alloy intersects that of nickel metal. With increasing nickel content the values of $c_{alloy/Ni}$ decrease linearly. At the same time the difference between c_{crit} and $c_{alloy/Ni}$ becomes progressively smaller and for Cu–40Ni alloy the values of c_{crit} and $c_{alloy/Ni}$ reach the same value, that is, 0.05 mol dm^{-3}.

It should be emphasised that, although copper also shows a break in the straight line for chloride concentrations higher than 0.5 mol dm^{-3}, we believe that this is a different effect from that observed for copper–nickel alloys. First, in this concentration range copper does not undergo typical localized corrosion attack, and, secondly, the constant b amounts to −0.09 V dec^{-1}, whereas for alloys an average value of −0.21 V dec^{-1} is obtained, which is almost identical to that for nickel metal, that is, −0.20 V dec^{-1}. As far as Cu–10Ni alloy is concerned, it is difficult to say which effect prevails, since the value of constant b lies between that of copper and nickel, that is, −0.11 V dec^{-1}.

Summarizing, E_c against c_{NaCl} diagrams determined from anodic polarization curves denote the regions where a particular material is protected against localized breakdown, and where it is susceptible to localized breakdown of the passive layer. With increasing chloride concentration the resistance of copper–nickel alloys to localized breakdown increases with increasing nickel content. This is due to the change in constant b, which for $c > c_{crit}$ becomes four times smaller and therefore similar to that of nickel metal.

3.3. *Analysis of corrosion products*

The results presented above prove that an increase in chloride concentration strongly influences the resistance of Cu–Ni alloys to localized corrosion. In the presence of a low chloride concentration (0.025 mol dm^{-3}) the current density measured for both nickel and Cu–40Ni and alloy starts to increase at potentials which are more negative than those of both copper and Cu–10Ni alloy (Figs 1–6). The nickel
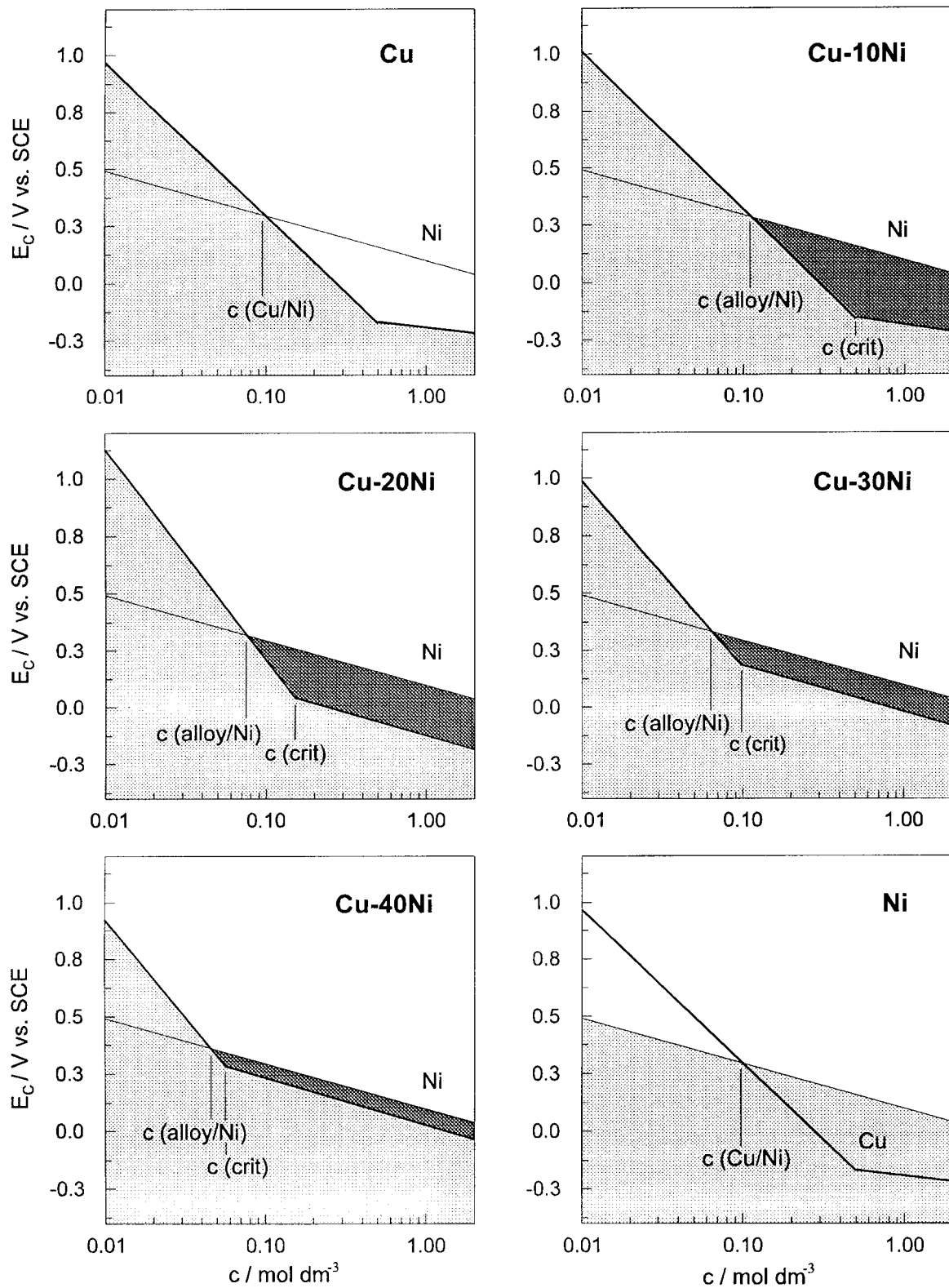
Fig. 7. E_c/c_{NaCl} diagrams for Cu metal, Cu–*x*Ni alloys and Ni metal. The critical potential E_c is determined from the anodic polarization curves (Figs 1–6) as the potential at which the current density reaches 1×10^{-4} A cm^{-2}. $c_{Cu/Ni}$ is the chloride concentration at which straight lines of copper and nickel intersect ($c_{Cu/Ni}$ = 0.1 mol dm^{-3}. c_{crit} denotes the chloride concentration at which the straight line $E_c = a + b \log c_{NaCl}$ changes its slope. $c_{alloy/Ni}$ is the chloride concentration at which the straight line of a particular alloy intersects that of nickel metal. For comparison, straight lines for nickel or copper are given.

surface is covered by round pits surrounded by a ring of pale yellow corrosion product retained after rinsing. Initially formed pits at the surface of Cu-40Ni alloy are rapidly covered by large patches of a voluminous green product. In the case of copper an in-crease in the current density is followed by the appearance of localized corrosion spots which are rapidly covered by a large amount of blue–green voluminous product. No apparent corrosion attack was identified for Cu–10Ni alloy.

More detailed information regarding the morphological and compositional changes at the electrode surface were obtained by SEM and EDS analyses (Figs 8–11). A typical image of a localized spot attacked on the nickel surface is given in Fig. 8(a). At the pit bottom nickel metal is identified. Pits of round shape are surrounded by the undissolved reaction product. Its morphology and composition are given in Fig. 8(b) and (c), respectively. The EDS spectrum identified this product as nickel oxide. No chloride signal was identified. It should be taken into account, however, that $NiCl_2.6H_2O$ is very soluble. Thus even if a certain amount was formed, it was dissolved more readily compared to the oxide, which remained at the surface.

Whereas no significant corrosion attack was observed for Cu–10Ni alloy, large patches of green corrosion product are formed on Cu–40Ni alloy. Its
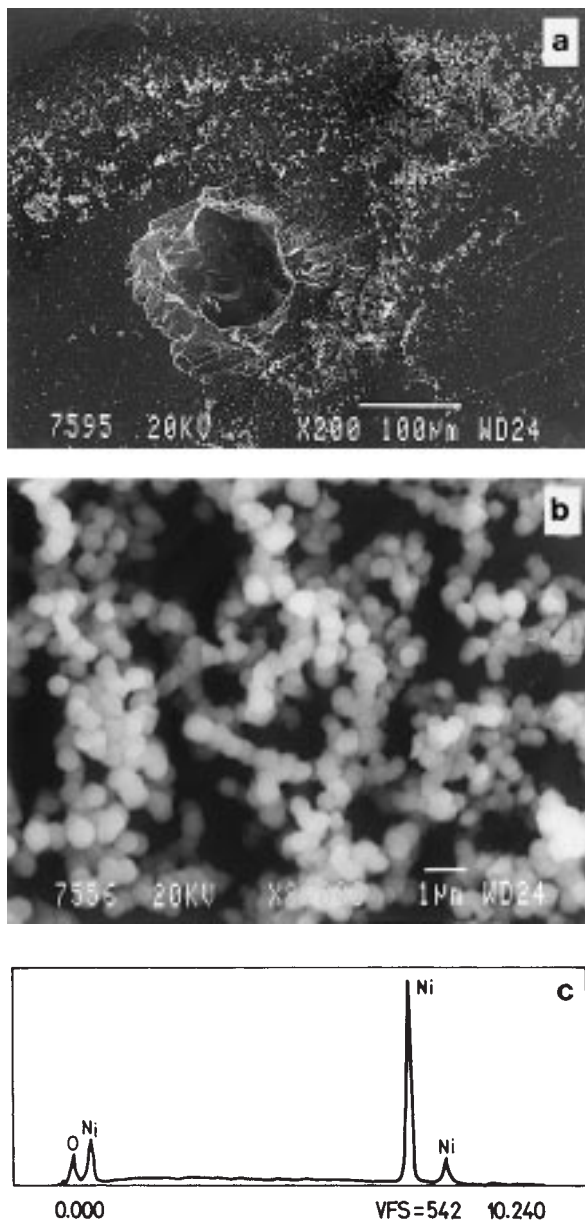
well defined grain structure and composition are given in Fig. 9(a) and (b), respectively. Considering that the content of Ni in the bulk alloy is 40 wt %, the corrosion product contains only a small amount of nickel (compare Fig. 9(b) and (c)). Obviously, the major product formed on Cu–40Ni alloy is cupric oxychloride, which contains a certain amount of incorporated nickel. The green colour of this oxychloride suggests the presence of cupric oxychloride $CuCl_2.3CuO.4H_2O$ (Brunswick green), or atacamite $CuCl_2.3Cu(OH)_2$.

The SEM image and EDS spectrum of the blue–green corrosion product precipitated on the surface of copper are depicted in Fig. 10. The EDS spectrum suggests that it may correspond to cupric oxychloride $CuCl_2.2CuO.4H_2O$. It exhibits a well defined grain structure, with grains sometimes growing together to form bigger clusters.

A quite different situation is encountered in the presence of high chloride concentrations. The breakdown potentials of copper and Cu–10Ni alloy are more negative than those of nickel and Cu–40Ni

Fig. 8. Round pits (a) formed on nickel after a polarization experiment in borate buffer containing $0.025\,mol\,dm^{-3}$ NaCl. Pits are surrounded by crystallites (b) of nickel oxide (c).
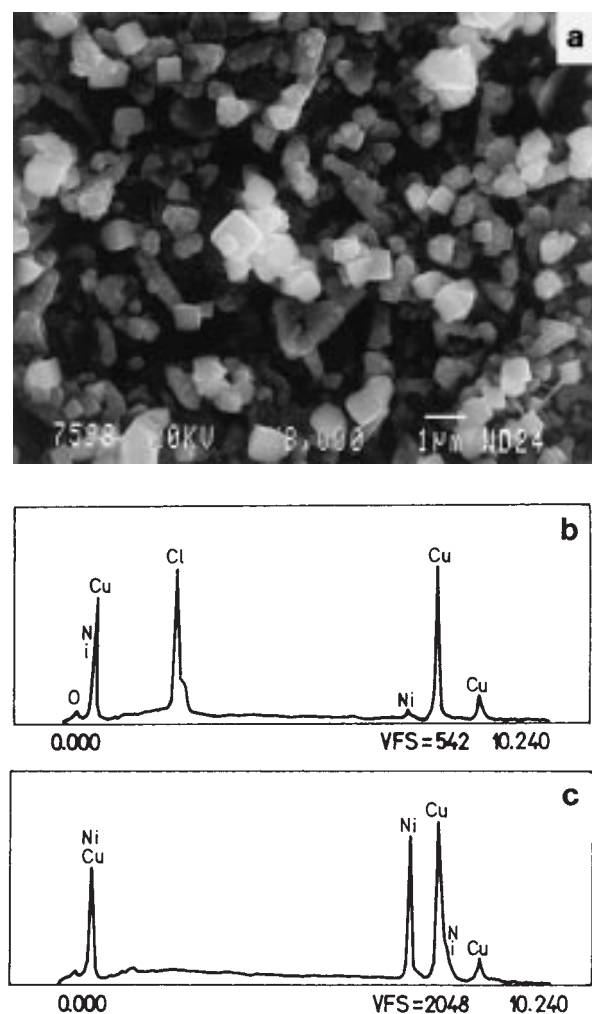

Fig. 9. SEM image (a) showing the well defined grain structure of a green corrosion product precipitated at the surface of Cu–40Ni alloy after a polarization experiment in borate buffer containing $0.025\,mol\,dm^{-3}$ NaCl. The EDS spectrum identifies it as cupric–nickel oxychloride (b). Compared to the bulk alloy (c), it contains little nickel.
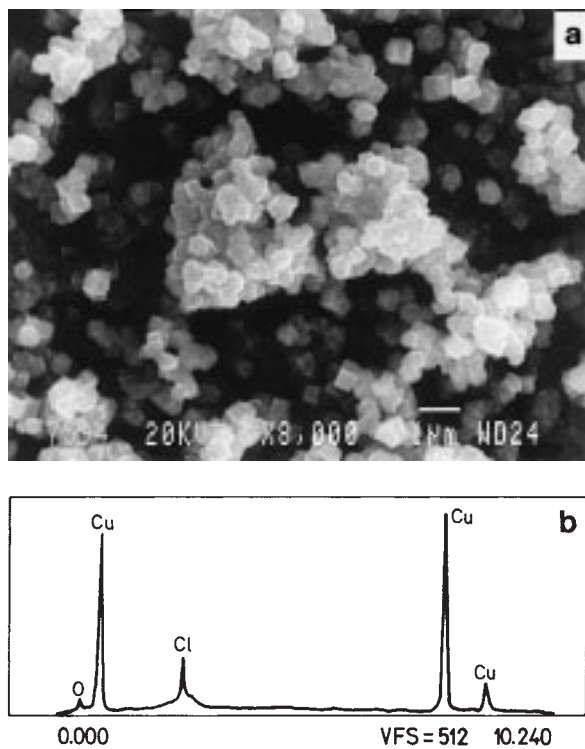
Fig. 10. Morphology (a) and composition (b) of the cupric oxychloride (blue–green) precipitated at the copper surface after a polarization experiment in borate buffer containing $0.025 \, mol \, dm^{-3}$ NaCl.
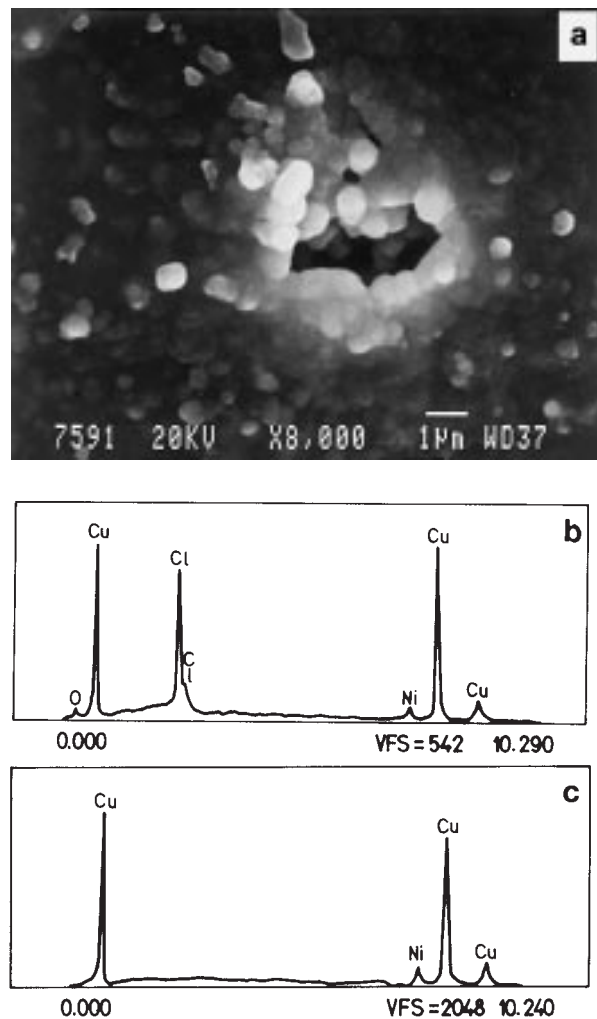
Fig. 11. SEM image (a) showing the grain structure of a green corrosion product precipitated at the surface of Cu–10Ni alloy after a polarization experiment in borate buffer containing $0.5 \, mol \, dm^{-3}$ NaCl. The EDS spectrum identifies it as cupric–nickel oxychloride (b). It contains a similar amount of nickel as the bulk alloy (c).

alloy (Figs 1–6). No corrosion product is formed at the surface of Ni and Cu–40Ni alloy in the presence of $0.5 \, mol \, dm^{-3}$ NaCl. In contrast, copper is covered by a red–orange homogeneous corrosion product and does not exhibit typical pitting corrosion. The corrosion attack on Cu–10Ni alloy starts at randomly distributed local points which rapidly decorate the whole surface. These spots are progressively covered by a large amount of a green corrosion product, forming patches at the surface. The detail in Fig. 11(a) illustrates the progressive coverage of the attacked spot by crystallites of corrosion product. As suggested by the EDS spectrum, this product corresponds to cupric oxychloride with a certain amount of incorporated nickel (Fig. 11(b)). The content of nickel does not differ significantly from that of the bulk alloy (Fig. 11(c)).

The EDS spectra in Figs 9(b) and 11(b) indicate that the composition of the corrosion product formed on Cu–10Ni and Cu–40Ni alloys is similar, that is, cupric oxychloride which contains a certain amount of nickel. Obviously, the amount of nickel incorporated in the layer is not strongly dependent on the nickel content in the bulk, since an increase to 40 wt % does not induce a corresponding increase of nickel signal in the corrosion product.

4. Conclusions

(i) The resistance of copper-nickel alloys to localized pitting attack is influenced by the chloride concentration range. There is a critical chloride concentration above which the resistance increase with increasing nickel content in the bulk alloy, and below which it increases with decreasing nickel content. Comparative measurements performed on pure metal constituents, that is, copper and nickel, explained this behaviour.

(ii) On the basis of potentiodynamic polarization curves, E_c against c_{NaCl} diagrams were created and three characteristic chloride concentrations are recognized: $c_{Cu/Ni}$, c_{crit} and $c_{alloy/Ni}$.

(iii) The concentration at which the straight lines of copper and nickel intersect is denoted as $c_{Cu/Ni}$, that is, $c_{Cu/Ni} \approx 0.1$ M. In the lower concentration range ($c < c_{Cu/Ni}$), copper exhibits a superior resistance to localized corrosion compared to nickel. However, since the constant b of nickel metal changes only slowly with increasing concentration, the situation becomes just the opposite as $c_{Cu/Ni}$ is exceeded. At higher chloride concentrations nickel exhibits a better resistance than copper.

(iv) The critical chloride concentration, c_{crit}, is related to the concentration at which the straight line of a particular alloy changes its slope. The concentration at which the straight line of a particular alloy intersects that of nickel is denoted as $c_{\text{alloy/Ni}}$. Both these concentrations decrease with increasing nickel content, although the second one to a higher extent.

(v) With increasing nickel content the difference between $c_{\text{alloy/Ni}}$ and c_{crit} becomes progressively smaller. Therefore, the critical concentration above which the alloy behaves similarly to nickel metal decreases. When the nickel content reaches 40 wt % , these two concentration become almost identical.

(vi) Although the behaviour of copper nickel alloys is strongly dependent on the nickel content, it seems that the composition of the precipitated outer layer is not greatly influenced by the bulk nickel content. For both Cu–10Ni and Cu–40Ni alloys corrosion attack is accompanied by the formation of green cupric oxychloride with a similar amount of incorporated nickel. It is thus reasonable to assume that the properties of the inner Cu_2O layer are mainly responsible for the corrosion resistance of copper-nickel alloys.

Acknowledgements

References

[1]   R. G. Blundy and M. J. Pryor, *Corros. Sci.* **12** (1972) 65.
[2]   R. F. North and M. J. Pryor, *Corros. Sci.* **10** (1970) 297.
[3]   H. Shih and H. W. Pickering, *J. Electrochem. Soc.* **134** (1987) 1949.
[4]   A. -M. Beccaria and J. Crousier, *Br. Corros. J.* **24** (1989) 49.
[5]   C. Kato, B. G. Ateya, J. E. Castle and H. W. Pickering, *J. Electrochem. Soc.* **127** (1980) 1897.
[6]   J. M. Popplewell and R. J. Hart, J. A. Ford, *Corros.* Sci. **13** (1973) 295.
[7]   R. Gasparini, C. Della Rocca and E. Ioannilli, *Corros. Sci.* **10** (1970) 157.
[8]   F. L. LaQue, *J. Am. Nav. Engrs.* **53** (1941) 29.
[9]   J. H. Sinfelt, J. L. Carter and D. J. C. Yates, *J. Catal.* **24** (1972) 283.
[10] M. M. Jakšić, *Electrochim. Acta* **29** (1984) 1539.
[11] K. Lohrberger and P. Kohl, *Electrochim. Acta* **29** (1984) 1557.
[12] H. Ezaki, M. Morinaga S. Watanabe and J. Saito, *Electrochim. Acta* **39** (1994) 1769.
[13] I. Milošev and Metikoš-Huković, *J. Electrochem. Soc.* **138** (1991) 61.
[14] *Idem, Corrosion* **48** (1992) 185.
[15] M. Metikoš-Huković and I. Milošev, *J. Appl. Electrochem.* **22** (1992) 448.
[16] H. -D. Speckmann, M. M. Lohrengel, J. W. Schultze and H. -H. Strehblow, *Ber. Bunsenges. Phys. Chem.* **89** (1985) 392.
[17] H. -H. Strehblow and B. Titze, *Electrochim. Acta* **25** (1980) 839.
[18] S. M. Abd El Halee and B. G. Ateya, *J. Electroanal. Chem.* **117** (1981) 309.
[19] M. R. G. de Chialvo, S. L. Marchiano and A. J. Arvia, *J. Appl. Electrochem.* **14** (1984) 165.